A Role for dNTP Binding of Human Immunodeficiency Virus Type 1 Reverse Transcriptase in Viral Mutagenesis†

Kellie K. Weiss,‡,§ Renxiang Chen,§,|| Mark Skasko,‡ Holly M. Reynolds,‡ Kwi Lee,‡ Robert A. Bambara,⊥ Louis M. Mansky,|| and Baek Kim*,‡

Department of Microbiology and Immunology, University of Rochester Medical Center, 601 Elmwood Avenue, Box 672, Rochester, New York 14642, Institute for Molecular Virology, University of Minnesota, 515 Delaware Street Southeast, Minneapolis, Minnesota 55455, and Department of Biochemistry and Biophysics, University of Rochester Medical Center, 601 Elmwood Avenue, Rochester, New York 14642

Received July 17, 2003; Revised Manuscript Received February 5, 2004

ABSTRACT: HIV-1 reverse transcriptase (RT) is a highly error prone DNA polymerase. We assessed whether the ability of RT to bind nucleotide substrates affects viral mutagenesis. Structural modeling predicts that the V148 and Q151 residues influence the interaction between RT and the incoming dNTP. When we introduce either a V148I or Q151N mutation, RT fidelity increases 8.7- or 13-fold, respectively, as measured by the M13 *lacZ*α forward mutation assay. Interestingly, pre-steady state kinetic studies demonstrated that these mutations do not alter polymerase fidelity during the first step of mutation synthesis, misincorporation. Rather, the V148I and Q151N mutations alter RT fidelity by weakening the ability of the polymerase to complete mismatch extension, the second step of mutation synthesis. While both these mutations minimally affect the binding of RT (K_D) to a mismatched template−primer complex (T/P), these mutant RTs are significantly impaired in their ability to bind (K_d) and chemically incorporate (k_{pol}) nucleotide substrate onto a mismatched T/P. These differences in binding and catalysis translate into 24- and 15.9-fold increase in mismatch extension fidelity for the V148I and Q151N RT mutants, respectively. Finally, we employed a cell-based pseudotyped HIV-1 mutation assay to determine whether changes in these dNTP binding residues alter RT fidelity *in vivo*. We found that the V148I and Q151N mutant viruses had 3.8- and 5.7-fold higher fidelities than wild-type viruses, respectively, indicating that the molecular interaction between HIV-1 RT and the dNTP substrate contributes to viral mutagenesis.

HIV-1 reverse transcriptase (RT)[1] is a highly error prone DNA polymerase (*1*, *2*). Although the lack of a 3′ → 5′ proofreading exonuclease contributes to the inaccurate nature of HIV-1 RT, this fact alone cannot account for the observed high error rate (*2*). Other retroviral RTs lacking proofreading capabilities (e.g., MuLV RT and AMV RT) have 10−18 times higher fidelity than HIV-1 RT (*3*), suggesting that the active site of HIV-1 RT must have evolved mechanisms for promoting mutagenesis.

The process of mutation synthesis involves two mechanistically distinct DNA polymerization events (*4*). The first step of mutation synthesis is a misincorporation event when a binary RT•T/P complex binds and chemically catalyzes the incorporation of an incorrect nucleotide. This generates a T/P product that is mismatched at the 3′ terminus of the primer strand. While polymerases associated with a 3′ → 5′ exonuclease are able to remove this mismatch, HIV-1 RT lacks this enzymatic activity and must therefore perform a second polymerization event called mismatch extension. This second step of mutation synthesis involves RT initially binding a mismatched T/P, followed by correct dNTP binding and chemical incorporation. RT fidelity is therefore defined by its ability to complete both of these events.

Pre-steady state kinetic assays can measure the kinetic parameters associated with each step of DNA polymerization: (1) polymerase binding to T/P (K_D), (2) subsequent binding of an incoming nucleotide (K_d), and (3) conformational change and/or chemical catalysis of the dNTP onto the primer strand [k_{pol} (*5*)]. Using these assays, we can assess the kinetic parameters associated with misincorporation or mismatch extension by measuring the extent of product formation when utilizing either a matched or mismatched T/P, respectively. Previous studies employing these techniques have shown that HIV-1 RT is relatively efficient at carrying out both these steps of mutation synthesis (*6*, *7*). The efficiency (k_{pol}/K_d) at which RT performs incorrect dNTP polymerization is considerably higher than that reported for

† This research was supported by Grants AI49781 (to B.K.), GM29573 (to R.A.B.), and GM56615 (to L.M.M.) and Training Grant AI07362-12 (to K.K.W.) from the National Institutes of Health.

* To whom correspondence should be addressed: Department of Microbiology and Immunology, University of Rochester Medical Center, 601 Elmwood Ave., Box 672, Rochester, NY 14642. Telephone: (585) 275-6916. Fax: (585) 473-9573. E-mail: baek_kim@urmc.rochester.edu.

‡ Department of Microbiology and Immunology, University of Rochester Medical Center.

§ These authors contributed equally to this work.

|| University of Minnesota.

⊥ Department of Biochemistry and Biophysics, University of Rochester Medical Center.

[1] Abbreviations: dNTP, 2′-deoxynucleoside 5′-triphosphate; T/P, template−primer complex; RT, reverse transcriptase; HIV-1, human immunodeficiency virus type 1; SIV, simian immunodeficiency virus; p66, 66 kDa HIV-1 RT polypeptide; SDS, sodium dodecyl sulfate.

10.1021/bi035258r CCC: $27.50
Published on Web 03/26/2004

other DNA polymerases involved in replication such as the exo$^-$ Klenow fragment (KF) of *Escherichia coli* DNA polymerase I and the exo$^-$ T7 DNA polymerase (*7*−*9*). Interestingly, HIV-1 RT is more capable of incorporating dNTPs onto a mismatched T/P than of incorporating incorrect nucleotides onto a matched T/P (*6*). Because HIV-1 RT lacks 3′ → 5′ exonuclease, its ability to carry out efficient mismatch extension will contribute to its error prone nature.

We previously identified a molecular interaction between RT and the nucleotide substrate that is crucial to the process of misincorporation. Our pre-steady state kinetic analysis of the Q151N RT mutant showed that alterations in this residue dramatically increased the fidelity of the polymerase such that incorrect nucleotide incorporation could not be assessed (*10*). In this study, we assessed the kinetic parameters associated with mismatch extension for the Q151N mutant. In addition, we performed a detailed analysis of our novel V148I mutant. The V148I mutant was originally identified from a molecular clone of SIV, and was found to increase the fidelity of SIV RT (*11*). Structural examination using the related HIV-1 RT model revealed that V148 lies near the Q151 residue and may actually influence RT fidelity by modulating the placement of Q151 in the RT active site. To verify if residue 148 is also important in HIV-1 RT fidelity, we measured the pre-steady state kinetic parameters associated with both steps of mutation synthesis, misincorporation and mismatch extension.

We report here that a mutation of residue 148 of HIV-1 RT alters the ability of the polymerase to bind incoming nucleotide substrates; however, unlike our previous studies with the SIV V148I and HIV-1 Q151N RT mutants, we were able to measure the kinetic parameters for misincorporation with our HIV-1 V148I RT (*10*, *11*). Interestingly, our results indicate that the V148I mutation does not significantly alter the ability of HIV-1 RT to differentiate between correct and incorrect nucleotides. A change in its ability to complete the second step of mutation synthesis, mismatch extension, was responsible for the observed changes in RT fidelity. A similar observation was made with the HIV-1 Q151N RT mutant. While changes in the binding of RT to the incoming dNTP dramatically altered the ability of the Q151N mutant to complete misincorporation events, a mutation at this residue also affected the efficiency at which it performed mismatch extension. As it is likely that HIV-1 RT fidelity contributes to viral genomic mutagenesis (*12*, *13*), the last experiment performed in this study was a cell-based pseudotyped HIV-1 mutation assay for measuring the fidelity of the V148I and Q151N mutants *in vivo*. We report here that the molecular interaction between HIV-1 RT and the incoming dNTP substrate plays an important role in HIV-1 mutagenesis.

EXPERIMENTAL PROCEDURES

Plasmids and Strains. HIV-1 RT was overexpressed in *E. coli* BL21 (Novagen) from pBK33 (*14*, *15*). This plasmid encodes full-length HXB2 wild-type p66 fused at the N-terminus to six histidine residues. *E. coli* NM522 (Stratagene) was used for the plasmid maintenance during the construction of pBK33 derivatives containing V148I and Q151N mutations.

Construction and Purification of Mutant HIV-1 RTs. The HIV-1 V148I RT mutant was created using PCR-based site-directed mutagenesis. Two primers were used to generate a PCR fragment flanked by restriction sites that are unique within pBK33: *Eco*RV (near codon 144) and *Bam*HI (near codon 155). The first primer containing an amino acid substitution (underlined) at residue V148 (5′-TTTTA**GATATC**AGTACAATATCCTTCCACAGGGATGGAAAGG-3′) encoded *Eco*RV (bold), and the second primer (5′-AAA**GGATCC**CCAGCAATATTCCAAAG-3′) had the *Bam*HI site (bold). The wild-type RT sequence in pBK33 was replaced with the digested product amplified with these two primers. Introduction of the V148I mutation was confirmed by DNA sequencing. Subsequently, the wild type, Q151N, or the resultant N-terminally His-tagged mutant V148I RT proteins were purified as previously described (*15*, *16*). From 1 L of culture, we were able to purify 2 mg of homodimeric p66−p66 HIV-1 RT with a purity of >95% as determined by visual inspection of Coomassie Blue-stained SDS−polyacrylamide gels.

M13mp2 lacZα Forward Mutation Assay. A mutant frequency for the HIV-1 V148I RT mutant was determined as previously described (*17*). Briefly, M13mp2 DNA containing a 361-nucleotide single-stranded gap was prepared. Gapped M13mp2 DNA (1 μg) was incubated with RT (250 nM), four dNTPs (250 μM each), 25 mM Tris-HCl (pH 8.0), 100 mM KCl, 2 mM DTT, 5 mM $MgCl_2$, and 0.1 mg/mL bovine serum albumin (New England Biolabs) at 37 °C for 20 min. Three independent gap filling reactions were performed for RT proteins. Production of double-stranded DNA was verified using a 0.7% agarose gel and then transformed into MC1016 cells. Transformed cells were then plated onto M9 plates containing X-gal, IPTG, and CSH50 lawn cells. Approximately 5000 plaques per gap filling reaction were analyzed. Mutant M13mp2 clones yield plaques that have an altered color (pale blue and clear). This was verified by sequencing the DNA isolated from a small number (four to six) of mutant plaques. All phage DNAs from the mutant plaques encoded mutations within the lacZα gene, indicating that mutations were generated during the gap filling reaction. The mutant frequency was therefore determined as a ratio of mutant (pale blue and clear) plaques to mutant and wild-type (dark blue) plaques.

Pre-Steady State Kinetic Assays. Pre-steady state burst and single-turnover experiments were performed to examine the transient kinetics associated with incorporating a single nucleotide onto either a matched or mismatched T/P. Both primers were annealed onto a 40-mer RNA template (5′-AAGCUUGGCUGCAGAAUAUUGCUAGCGGGAAUUCGGCGCG-3′). The matched primer is a 16-mer ^{32}P-labeled T primer (5′-CGCGCCGAATTCCCGC-3′), and the mismatched primer is a 16-mer ^{32}P-labeled G/T primer (5′-CGCGCCGAATTCCCGT-3′). The primers are identical except that the 3′ nucleotide on the G/T primer is not complementary to the template nucleotide, which is representative of a mismatched T/P product formed after a misincorporation event. We can therefore use the G/T mismatch primer to measure the kinetics of mismatch extension. Reactions were performed as previously described using a Kintek rapid quench machine (*7*, *10*, *18*). Products were analyzed by 14% denaturing sequencing gel electrophoresis and quantified with the Cyclone PhosphorImager (Perkin-Elmer Life Sciences).

Pre-steady state burst experiments were employed to determine the active site concentrations of the RT proteins on both matched and mismatched T/Ps. In these experiments, 800 μM TTP was rapidly mixed with RT (75 or 150 nM as determined with a Bradford assay, Bio-Rad, Richmond, CA) bound to T/P (150 nM). In the pre-steady state single-turnover experiments, active RT (as determined by the burst experiments) was added in excess of T/P. These experiments were used to determine the dNTP concentration dependence of the purified HIV-1 RT proteins. When correct TTP incorporation was examined with either matched or mismatched T/P, 50 nM (or 400 nM) active RT and 40 nM T/P were used. In reactions involving incorrect dNTPs, experiments were carried out manually and at longer time points with higher concentrations of RT (400 nM). We also employed 50 nM wild-type RT for the k_{obs} determination with incorrect dNTPs, which gave much weaker product signals than the reactions with 400 nM RT. However, the kinetic parameters obtained from low and high RT concentrations were very similar (data not shown).

Data Analysis. Pre-steady state kinetic data were analyzed using nonlinear regression. Equations were generated with KaleidaGraph version 3.51 (Synergy Software). Data points obtained during the burst experiment were fitted to the burst equation (eq 1) (*5*, *18*)

$$[\text{product}] = A[1 - \exp(-k_{obs}t) + k_{ss}t] \quad (1)$$

where A is the amplitude of the burst, which reflects the actual concentration of the active form of the enzyme, k_{obs} is the observed first-order rate constant for dNTP incorporation, and k_{ss} is the observed steady state rate constant (*7*, *18*, *19*). Data from single-turnover experiments were fit to a single-exponential equation that measures the rate of dNTP incorporation (k_{obs}) per given dNTP concentration ([dNTP]). These results can then be used to determine K_d, the dissociation constant for binding of dNTP to the RT·T/P binary complex, and k_{pol}, the maximum rate of chemical catalysis. This was done by fitting the data to the following quadratic equation (eq 2)

$$k_{obs} = k_{pol}[\text{dNTP}]/(K_d + [\text{dNTP}]) \quad (2)$$

From this equation, we could then identify the kinetic constants for each RT during pre-steady state kinetics: k_{pol}, the maximum rate of dNTP incorporation, and K_d, the equilibrium dissociation constant for the interaction of dNTP with the E·DNA complex (*18*, *20*).

Determination of T/P Binding Affinity. Reactions to determine the T/P concentration dependence of the RT proteins were also performed using the rapid quench machine. In these experiments, 50 nM RT (or 400 nM) was preincubated with varying concentrations of T/P (from 10 to 700 nM). Polymerization was initiated by addition of 800 μM TTP and allowed to proceed at 37 °C for 250 ms. The extent of product formation was measured and fit to the following quadratic equation (eq 3):

$$[\text{RT·T/P}] = 0.5(K_D + [\text{RT}]_t + [\text{T/P}]) - 0.5\sqrt{(K_D + [\text{RT}]_t + [\text{T/P}])^2 - 4[\text{RT}]_t[\text{T/P}]} \quad (3)$$

where [RT·T/P], K_D, $[RT]_t$, and [T/P] represent the productive RT·template concentration, the equilibrium dissociation constant for binding of RT to T/P, the active RT concentration (see Figure 1), and the total T/P concentration, respectively. From eq 3, the K_D values for binding of wild-type and mutant RTs to the aforementioned T/P were determined (*21*).

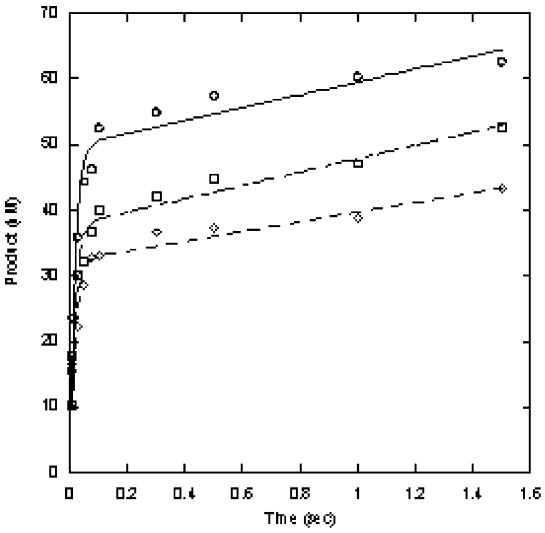

FIGURE 1: Pre-steady state kinetic TTP incorporation of RT proteins on a matched T/P. Pre-steady state and steady state kinetics of wild-type (○), V148I (□), and Q151N (◇) HIV-1 RTs incorporating correct TTP onto a matched T/P. Reactions were carried out at the indicated times by mixing together prebound RT (protein concentration of 75 nM as determined with a Bradford assay)·T/P complex (150 nM) with 800 μM dTTP under rapid quench conditions (see Experimental Procedures). The data were fit into the burst equation (eq 1) as indicated by the solid line, which provides a measure of the active concentration of RT (A), the observed first-order rate constant for the burst phase (k_{obs}), and the first-order rate constant for the linear phase (k_{ss}) of each RT on the matched T/P. (○) The active concentration (A) of wild-type HIV-1 RT was 49.7 ± 9.3 nM. Its k_{obs} was 56.4 ± 9.8 s^{-1}, and its k_{ss} was (19.7 ± 6.3) × 10^{-2} s^{-1}. (□) The active concentration (A) of the V148I HIV-1 RT was 32.3 ± 10.1 nM. Its k_{obs} was 58.2 ± 11.5 s^{-1}, and its k_{ss} was (22.8 ± 7.6) × 10^{-2} s^{-1}. (◇) The active concentration (A) of the Q151N HIV-1 RT was 37.6 ± 8.7 nM. Its k_{obs} was 59.3 ± 5.0 s^{-1}, and its k_{ss} was (27.1 ± 8.3) × 10^{-2} s^{-1}.

Retroviral Vectors and Expression Plasmids. The HIV-1 vector used in these studies was previously described (*22*, *23*). The vector cassette containing the *lac*Z gene, an internal ribosomal entry site (IRES) element, and the neomycin phosphotransferase gene (*neo*) were introduced into pGEM NL4-3 (full-length molecular clone of NL4-3) to create pHIVLacZ-IRES-neo. To produce vector virus, the HIV-1 vector was complemented *in trans* with pSVgagpol-rre-MPMV, the amphotropic murine leukemia virus *env* expression plasmid, pSV-A-MLV-env, and a Vpr expression plasmid derived from pAS1B (*24*, *25*). The RT variants analyzed in these experiments were constructed by a primary combinatorial, two-step polymerase chain reaction (PCR) protocol (*26*, *27*) or by using the Quickchange XL mutagenesis kit (Stratagene). All RT variants that were made were sequenced to verify the proper introduction of mutations.

Transfections, Infections, and Cocultivations. The COS-1 and HeLa cell lines were obtained from the American Type Culture Collection (Rockville, MD) and were maintained in Dulbecco's modified Eagle's medium containing 10% fetal bovine serum and 10% calf serum, respectively. HIV-1 vector and expression plasmids were transfected into HeLa cells

Table 1: M13mp2 *lacZ*α Forward Mutation Assay with HIV-1 RT Proteins

RT	total no. of plaques	no. of mutant plaques	mutant frequency ($\times 10^{-3}$)
wild type[a]	11420	298	26.1
V148I	9880	29	3.0 ($\times$8.7)[b]
Q151N[a]	13520	27	2.0 ($\times$13)[b]

[a] Data previously published (*16*). [b] Fold decrease relative to wild-type HIV-1 RT.

by using Superfect (Qiagen). HeLa cells were infected in the presence of Polybrene (*13*). Infection of HeLa target cells was also done by cocultivation of virus-producing cells and target cells (*13*).

Experimental Protocol for Generating a Single Round of HIV-1 Vector Replication. The experimental protocol developed to generate a single round of HIV-1 vector replication has previously been described (*13*). In this protocol, HeLa cells containing the HIV-1 vector provirus were created by transiently tranfecting the HIV-1 vector and helper plasmids into COS-1 cells, harvesting virus 2 days post-transfection, and infecting HeLa cells. G418-resistant clones were isolated and characterized for the presence of single proviruses. The cells were also stained with X-gal to ensure that no mutations had occurred in the *lac*Z gene. Selected clones were then used to generate a single round of HIV-1 vector replication. HeLa cell clones with single integrated proviruses were transiently transfected with helper plasmids and were treated with mitomycin C 48 h post-transfection, and then mixed with fresh HeLa cells. G418-resistant cells resulting from virus infection of fresh HeLa cells were selected, and cells were then stained with X-gal. The ratio of white and light blue stained colonies to total colonies observed provided a forward mutant frequency. In each experiment, similar numbers of colonies were screened for control and experimental samples. Titers for control experiments (wild-type RT) were typically 500−1000 colony-forming units (cfu) per 5×10^5 target cells.

RESULTS

*M13mp2 lacZ*α *Forward Mutation Assay*. This method measures the mutant frequency associated with the DNA-dependent DNA polymerase (DDDP) activities of polymerases. When a polymerase (e.g., RT) copies a portion of the *lacZ*α gene, mutations that are generated are identified by the number of plaques with altered color phenotype (pale blue or clear) when the product is expressed in a specific indicator strain. A value of mutant frequency, which is the ratio of mutant (pale blue and clear) plaques to mutant and wild-type (dark blue) plaques, can be determined and will provide a measure of the overall fidelity of a particular RT. When we examined HIV-1 V148I RT, the mutant exhibited an 8.7-fold lower mutant frequency than wild-type RT (Table 1). This result is consistent with published data obtained using a gel-based misincorporation assay (*11*). It should also be noted that a mutation in residue 148 altered HIV-1 RT fidelity less severely than changes in residue Q151 (*16*).

Pre-Steady State Burst Kinetics and Active Site Concentrations of HIV-1 RT Proteins. Because polymerase activity varies when different T/Ps are used, we assessed the active concentration of each RT employed in this study using both matched and mismatched T/Ps. To determine the active concentration, we assessed the pre-steady state product formation when T/P (150 nM) is in excess of RT protein (Bradford assay concentration of 75 nM) using quench flow. As shown in Figure 1, we observed a typical burst of product formation corresponding to incorporation of TTP onto T/P prebound with enzyme (<100 ms). This is followed by a rate transition to a slower steady state linear phase that reflects the rate-limiting product release step (>150 ms). Using eq 1, we can measure the amount of active enzyme, the burst rate (k_{obs}), and the steady state kinetic rate (k_{ss}). By comparing the amount of active enzyme with the input concentration, we were able to determine the percentage of active enzyme in our enzyme preparation, and the actual concentration of active RT in the reaction. In these burst experiments, we used 800 μM TTP to provide a near-saturation concentration of TTP for the V148I and Q151N mutant proteins that were predicted to have much higher K_d values for binding to TTP than the wild-type RT protein (i.e., >200 μM for the K_d of Q151N). On the matched T/P (Figure 1), our results indicate that 49.7 nM (66.3%) wild type, 32.3 nM (43.1%) V148I, and 37.6 nM (50.1%) Q151N RT proteins were active. To confirm the calculated RT active site concentrations, we also employed 150 nM RT (protein concentration), which gave lower ratios (1:1.5 to 1:1.9) between active RT and T/P than the 75 nM RT reactions (1:3.0 to 1:4.6, Figure 1). The percentages of the active site concentrations determined with 150 nM RT (53−68%) were very similar to those with 75 nM RT. However, the biphasic transition from the pre-steady state to the steady state (Figure 1) appeared to be less dramatic in the experiment with 150 nM RT (data not shown).

Pre-Steady State Kinetics of Incorporation of a Correct dNTP onto a Matched T/P. By analyzing the dependence of the reaction rate (k_{obs}) on dNTP concentration, we can obtain a measure of both the maximum rate of dNTP incorporation (k_{pol}) and the dNTP binding affinity (K_d) after fitting the data to a hyperbolic curve (eq 2, Figure 2). Using wild-type, V148I, and Q151N RT proteins (50 or 400 nM) with 40 nM matched T/P, we first determined the rate of product formation corresponding to correct TTP (0.25−300 μM) incorporation. Even though an excess of active RT (50 nM) over T/P was used, because of the low affinity of RT proteins for the T/P (see Table 4), this reaction condition likely allowed both a single round and multiple rounds of TTP incorporation. For this reason, we determined the kinetic parameters (K_d and k_{pol}) of each RT protein by using the k_{obs} values that were obtained at different TTP concentrations during the single-turnover burst reaction. To confirm these values, we also examined the K_d and k_{pol} values of the three RT proteins with a higher active RT concentration (400 nM), which allows approximately 70% of the T/P to bind to the RT proteins. This experiment also yielded kinetic values similar to those determined with 50 nM RT (Table 2, TTP); the K_d values for binding of the wild type, V148I, and Q151N RTs to TTP were 1.1, 29.9, and 276.8 μM, respectively, and k_{pol} values of the wild type, V148I, and Q151N RTs were 22.8, 23.5, and 26.6 s^{-1}, respectively.

As shown in Table 2, we see that alterations of residue 148 (Val → Ile) and residue 151 (Gln → Asn) have only a small apparent effect on the maximum rate at which HIV-1 RT incorporates correct TTP (k_{pol}). The k_{pol} for wild-type

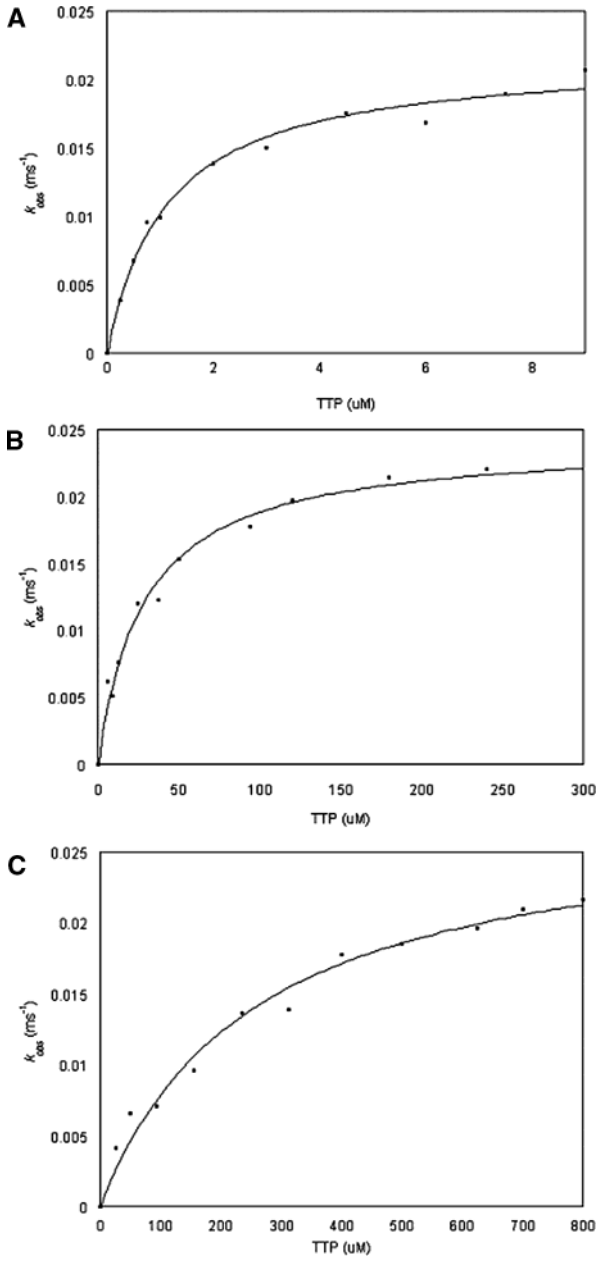

FIGURE 2: TTP concentration dependence on a matched T/P. k_{obs} values of wild-type (A), V148I (B), and Q151N (C) HIV-1 RT proteins were determined at different TTP concentrations with 50 nM active RT and 40 nM T/P. Higher TTP concentrations were used for the V148I and Q151N protein reactions because of their increased K_d values. The k_{pol} and K_d values were calculated by fitting these results to eq 2 and are listed in Table 2.

RT was 21.7 s^{-1}, and the values for the V148I and Q151N mutants were 24.2 and 28.1 s^{-1}, respectively. In contrast, mutations in these residues greatly alter the ability of the RTs to bind correct TTP. We observed a 26-fold decrease in the binding affinity for the V148I protein (28.5 μM) and a 229-fold decrease with the Q151N mutant (257.6 μM) as compared to that of wild-type RT (1.1 μM). These results for correct TTP incorporation with wild-type HIV-1 RT are similar to those reported for correct dCTP (*7*, *20*) and dATP incorporation (*10*).

Pre-Steady State Kinetics of Incorporation of an Incorrect dNTP onto a Matched T/P. We then assessed the pre-steady state kinetic parameters associated with incorporation of an incorrect nucleotide onto a matched T/P with the wild-type, V148I, and Q151N HIV-1 RT proteins (Table 2). When either an incorrect dCTP or dGTP was incorporated onto our matched T/P, the ability of wild-type RT to carry out both kinetic steps of nucleotide binding (K_d) and conformational change or chemical catalysis (k_{pol}) was weakened compared to correct TTP incorporation. The same was true for the V148I RT mutant. In the case of incorrect dGTP incorporation, the k_{pol} values for wild-type and V148I RTs were 0.037 and 0.020 s^{-1}, respectively. Similarly, the k_{pol} for wild-type RT with dCTP was 0.027 s^{-1} and for V148I was 0.024 s^{-1}. These results illustrate that although the k_{pol} step of both RTs is slower than when correct nucleotides are utilized, the V148I mutation does not alter the ability of HIV-1 RT to complete the k_{pol} step of misincorporation. Rather, initial observations suggest that this mutation affects the binding of RT to the nucleotide substrate. From Table 2, we can see that with dGTP, V148I RT (328.8 μM) has a 24-fold lower binding affinity than the wild-type RT (13.8 μM). When dCTP is utilized, V148I RT (1055 μM) exhibits a 9-fold lower binding affinity than wild-type RT (117.3 μM). The fact that the V148I mutation reduces RT's binding affinity (K_d) for both correct and incorrect dNTPs to a similar degree suggests that the interaction between residue 148 and the nucleotide substrate is generally consistent. There are kinetic consequences associated with this phenomenon that will be addressed later in this section.

As in our previously published HIV-1 Q151N RT study (*10*), we were unable to measure the kinetics associated with incorrect dNTP incorporation. The reaction rate for incorrect dGTP and dCTP incorporation (k_{obs}) increased in a linear fashion up to a substrate concentration of even 4 mM. So although saturating concentrations of both dGTP and dCTP must be greater than 4 mM, higher dNTP concentrations could not be used because they inhibit RT activity (*9*). Substrate inhibition at dGTP and dCTP concentrations of >4 mM precluded measuring the kinetic values of k_{pol} and K_d for misincorporation events. We can only conclude that the Q151N mutation reduces the affinity of RT for the incoming dNTP such that the K_d of the RT for incorrect dGTP and dCTP could be near millimolar ranges. However, we attempted to estimate minimum k_{pol} values for the Q151N mutant (i.e., k_{obs} at 4 mM dNTP). At incorrect dNTP concentrations of 4 mM, Q151N RT incorporates incorrect dGTP and dCTP at rates of 1.6×10^{-3} and 4.6×10^{-3} s^{-1}, respectively. While this rate of dCTP incorporation is comparable to that seen with wild-type RT (0.037 s^{-1}), Q151N RT is 23.1-fold slower at incorporating incorrect dGTP. In conjunction with their K_d differences (minimum millimolar ranges for Q151N RT with dCTP and dGTP), we can estimate that the Q151N mutant RT is 191.7- and 6750-fold less efficient (k_{pol}/K_d) than wild-type HIV-1 RT at carrying out dCTP and dGTP misincorporation reactions, respectively.

Traditionally, misinsertion fidelity is defined as the efficiency with which a polymerase differentiates correct nucleotides relative to incorrect (see eq 4 in Table 2). A high-fidelity polymerase is one that incorporates incorrect nucleotides very inefficiently such that this ratio would be very high. For V148I to be a high-fidelity polymerase, its misinsertion fidelity on matched T/P must be greater than that measured with wild-type RT. As shown in Table 2 (misinsertion fidelity), this is not the case. In the case of

Table 2: Pre-Steady State Kinetic Parameters of Wild-Type, V184I, and Q151N HIV-1 RT

dNTP	RT	k_{pol} (s^{-1})	K_d (μM)	k_{pol}/K_d (μM^{-1} s^{-1})	misinsertion fidelity[a]
TTP (correct)	wild type	21.7 ± 0.7	1.1 ± 0.1	19.7	–
	V148I	24.2 ± 0.7 ($\times 1.1$)[b]	28.5 ± 3.0 ($\times 25.6$)[b]	0.85 ($\times 23.2$)[b]	–
	Q151N	28.1 ± 1.8 ($\times 1.3$)[b]	257.6 ± 42.6 ($\times 234.2$)[b]	0.11 ($\times 179.1$)[b]	–
dGTP (incorrect)	wild type	0.037 ± 0.001	13.8 ± 2.2	2.7×10^{-3}	7297.3
	V148I	0.020 ± 0.002 ($\times 1.9$)[b]	326.3 ± 26.5 ($\times 23.6$)[b]	6.1×10^{-5} ($\times 44.2$)[b]	13935.4 ($\times 1.9$)[b]
	Q151N	$(1.6 \pm 0.9) \times 10^{-3}$[c] ($\times 23.1$)[b]	4000[d] ($\times 289.9$)[b]	4.0×10^{-7}[c] ($\times 6750$)[b]	275001.0[c] ($\times 37.7$)[b]
dCTP (incorrect)	wild type	0.027 ± 0.001	117.3 ± 7.3	2.3×10^{-4}	85653.2
	V148I	0.024 ± 0.002 ($\times 1.1$)[b]	1055 ± 131.2 ($\times 9.0$)[b]	2.3×10^{-5} ($\times 10$)[b]	36957.5 ($\times 2.3$)[b]
	Q151N	$(4.6 \pm 0.8) \times 10^{-3}$[c] ($\times 5.9$)[b]	4000[d] ($\times 34.1$)[b]	1.2×10^{-6}[c] ($\times 191.7$)[b]	91667.7[c] ($\times 1.1$)[b]

[a] $(k_{pol}/K_d)_{correct} + (k_{pol}/K_d)_{incorrect}/(k_{pol}/K_d)_{incorrect}$ (eq 4). [b] Fold change relative to wild-type HIV-1 RT. [c] Values determined by utilizing the k_{obs} as k_{pol} at 4 mM incorrect dNTP. [d] Minimum K_d, the highest concentration of dNTP used in this study.

Table 3: Pre-Steady State Kinetic Parameters of Wild-Type, V184I, and Q151N HIV-1 RT on Mismatched T/P

dNTP	RT	k_{pol} (s^{-1})	K_d (μM)	k_{pol}/K_d (μM^{-1} s^{-1})	mismatch extension fidelity[a]
TTP (correct)	wild type	$(0.5 \pm 5.6) \times 10^{-3}$	14.1 ± 0.6	0.04	493.5
	V148I	$(24.1 \pm 0.8) \times 10^{-3}$ ($\times 20.7$)[b]	344.7 ± 27.1 ($\times 24.4$)[b]	7.0×10^{-5} ($\times 571.4$)[b]	12143.9 ($\times 24.4$)[b]
	Q151N	$(17.3 \pm 0.5) \times 10^{-3}$ ($\times 28.9$)[b]	1218.0 ± 80.9 ($\times 86.4$)[b]	1.4×10^{-5} ($\times 2857.1$)[b]	7858.1 ($\times 15.9$)[b]

[a] $(k_{pol}/K_d)_{matched} + (k_{pol}/K_d)_{mismatched}/(k_{pol}/K_d)_{mismatched}$ (eq 5). [b] Fold difference in fidelity relative to wild-type HIV-1 RT.

incorrect dGTP incorporation, V148I RT has an only 1.9-fold higher fidelity than wild-type RT. Similarly, this mutant RT incorporates incorrect dCTPs with a 2.3-fold lower fidelity than the wild-type RT. Because changes in residue 148 concomitantly alter RT's ability to bind both correct and incorrect nucleotides, RT misinsertion fidelity is not significantly altered and cannot account for the observed 8.7-fold increase in V148I RT fidelity as measured by the M13 *lac*Zα forward mutation assay. Presumably, the V148I mutation does not alter RT fidelity during the first step of mutation synthesis, misincorporation.

Using our estimated efficiency values for the Q151N mutant to calculate its misinsertion fidelity with incorrect dCTP and dGTP, we see that the scenario with this mutant is somewhat akin to the observations made with the V148I RT. Both the mutant RTs have higher misinsertion fidelity for incorrect dGTP incorporation, with the difference between Q151N and wild-type RTs being more distinctive (37.7-fold difference); however, it should be noted that this difference in misinsertion fidelity is inflated. The efficiency of incorrect dGTP incorporation was calculated using k_{obs} at a dGTP concentration of 4 mM, which occurs within a linear range of dNTP dependence. It is likely that the k_{pol} of Q151N RT during dGTP incorporation is higher than the listed k_{obs}, which would translate into a diminished misinsertion fidelity value. In the case of incorrect dCTP incorporation, although Q151N RT does not have a lower misinsertion fidelity than wild-type RT like V148I RT, the misinsertion fidelity of Q151N RT for dCTP is only 1.1-fold higher than that of wild-type HIV-1 RT. So not unlike V148I RT, Q151N RT does not consistently have a higher misinsertion fidelity than wild-type RT. Our estimated calculations for misincorporation fidelity predict that our Q151N mutant RT does not discriminate between correct and incorrect nucleotides as defined by the traditional definition for misinsertion fidelity.

Pre-Steady State Kinetics of Incorporation by HIV-1 RT Proteins on a Mismatched T/P. Since the misinsertion fidelity data indicate that residue 148 does not influence HIV-1 RT fidelity during the incorporation event, we reasoned that the high-fidelity V148I mutant might be altered in its ability to complete the second step of mutation synthesis. We therefore measured the pre-steady state kinetic parameters for mismatch extension. In these experiments, we examined incorporation of TTP onto a mismatched T/P. Using 50 nM active RT as determined by mismatched T/P burst experiments with 40 nM mismatched T/P, we assessed product formation in the presence of varying concentrations of TTP (from 9 μM to 3 mM). The active site titration curve of wild-type HIV-1 RT with the mismatched T/P showed a typical biphasic response, fast pre-steady state and slow rate-limiting steady state incorporation reactions, as observed in the dNTP incorporation with the matched T/P (Figure 1). However, the mismatch T/P reaction curves for Q151N and V148I RTs appeared to be less biphasic (data not shown), suggesting that the step before or at the chemistry step may be rate-limiting in the mismatch extension reactions by these two RT mutants.

We fit the data into a quadratic equation (eq 2) and measured the K_d (dNTP binding) and k_{pol} (conformational change or chemical catalysis) values for the wild-type, V148I, and Q151N RT proteins (Figure 3). As shown in Table 3, wild-type RT is less efficient at both K_d and k_{pol} steps of the incorporation of TTP onto a mismatched T/P than polymerization using a matched T/P. The mutations at residues 148 and 151 appear to further weaken the ability of RT to carry out mismatch extension. Both the V148I and Q151N mutants are less capable of carrying out the K_d and k_{pol} steps of the TTP incorporation onto a mismatched T/P than wild-type RT. V148I RT is 24.4-fold (344.7 μM) and 20.7-fold (24.1×10^{-3} s^{-1}) less efficient at both K_d and k_{pol} steps, respectively, of the TTP incorporation with a mismatched T/P, and Q151N RT is 86.4-fold (1218.0 μM) and 28.9-fold (17.3×10^{-3} s^{-1}) less efficient, respectively. These changes in binding and conformational change or chemical catalysis translate into increases in their mismatch extension fidelities. When comparing efficiencies (eq 5 in Table 3) of correct nucleotide incorporation on a matched T/P to that on a mismatched T/P, we see that V148I RT has a 24.4-fold (12 143.9) and Q151N RT a 15.9-fold (7858.1) higher fidelity than wild-type RT (492.5). From these results, we can form two conclusions. (1) Since the fidelity ratio for wild-type HIV-1 RT to perform mismatch extension is actually lower

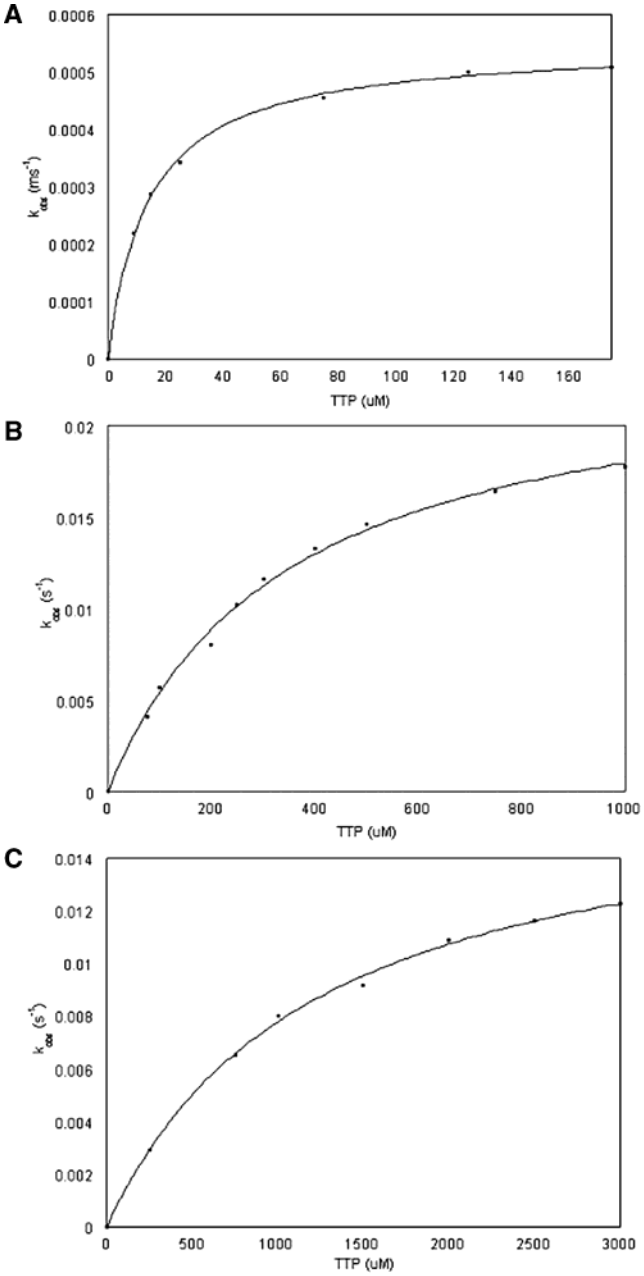

FIGURE 3: TTP concentration dependence on a mismatched T/P. k_{obs} values of wild-type (A), V148I (B), and Q151N (C) HIV-1 RT proteins were determined at different TTP concentrations with 400 nM active RT and 40 nM T/P. Higher TTP concentrations were used for the V148I and Q151N protein reactions because of their increased K_d values. The k_{pol} and K_d values were calculated by fitting these results to eq 2 and are listed in Table 3.

than its fidelity ratio when incorporating incorrect nucleotides, mismatch extension contributes to HIV-1 RT fidelity. (2) A mechanism by which the V148I and Q151N mutants alter polymerase fidelity is weakening the ability of RT to complete mismatch extension.

Affinity of RT Proteins for T/P. Since RT binding onto T/P precludes dNTP incorporation and is a mechanistic step that may contribute to the overall fidelity of a polymerase, we sought to measure how the V148I and Q151N mutations affected this T/P binding event. For this, we determined the affinity (K_D) of the mutant proteins for both our matched T primer and mismatched G/T primer annealed onto an RNA template. Using 50 nM active RT (as determined above using the appropriate T/P) with 800 μM TTP, we assessed product formation corresponding to a constant reaction time of 250 ms in the presence of varying concentrations of T/P. In our pilot experiments, the K_D values for binding of wild-type RT to the matched T/P were determined at both the 50 and 250 ms time points, where mainly single-turnover burst reactions occur. K_D values observed at both time points were very similar; however, the 250 ms experiments yielded less variability than those carried out at 50 ms.

Table 4: Constants (K_D) for Binding of HIV-1 RT Proteins to T/P

	K_D (nM)[a]		
T/P	wild type	V148I	Q151N
matched	198.5 ± 2.4	131.7 ± 6.1	144.6 ± 4.9
mismatched	53.8 ± 2.8	183.4 ± 6.2	203.2 ± 7.6

[a] K_D values were obtained using eq 3 as described previously (*21*).

From the binding curves (eq 3), we were able to obtain a measure of T/P binding affinity (K_D) for each RT protein. As seen in Table 4, wild-type RT has a K_D of 198.5 nM on a matched T/P. V148I and Q151N RTs have K_D values of 131.7 and 144.6 nM, respectively. These T/P binding affinity values with a matched T/P are comparable to the K_D of 90 nM for wild-type RT for a matched T/P previously reported by Vaccaro *et al.* (*28*). Some studies reported low K_D values for HIV-1 RT (*29*, *30*). This may result from the shorter length of the primer used in this study, which may provide fewer RT interactions with T/P than longer primers.

When using a mismatched T/P, wild-type, V148I, and Q151N RTs have binding affinities (K_D) of 53.8, 183.4, and 157.4 nM, respectively. While a small difference in mismatched T/P binding affinity exists between the wild-type and mutant RTs, the overall similarity in the affinities of these proteins for both matched and mismatched T/P suggests that RT residues 148 and 151 do not contribute significantly to this initial T/P binding step in DNA polymerization. These findings suggest that these mutations (1) do not alter RT fidelity by modulating the binding of the polymerase and the T/P during either the misincorporation or mismatch extension event and (2) do not substantially alter the geometry within the T/P binding site.

Analysis of HIV-1 RT Single-Amino Acid Variants (V148I and Q151N) on Virus Mutant Frequencies. The final experiment performed in this study was a cell-based HIV-1 mutagenesis assay for assessing the fidelity of the mutant RTs *in vivo*. Previously, we showed that an HIV variant containing the Q151N mutant RT had a virus mutant frequency that was one-fifth of that seen with wild-type HIV-1 during one round of HIV-1 replication (*13*). Employing the same cell culture fidelity assay, we report that the V148I RT variant has a virus mutant frequency that is approximately one-fourth of that observed with the wild type (Table 5). These results indicate that mutations at residues 148 and 151 can influence the accuracy of viral replication *in vivo*. The V148I variant showed a virus mutant frequency that was not significantly different from that of the Q151N variant. However, the trend suggests that the V148I RT may have a lower mutant frequency than Q151N RT, which was what we observed in the M13 *lac*Zα forward mutation assay. On the basis of these observations, it is also likely that the nucleotide binding changes during misincorporation (for Q151N) and the overall increase in mismatch extension

Table 5: Influence of HIV-1 RTs on *in Vivo* Virus Mutant Frequencies in One Round of Replication

RT	average mutant frequency ($\times 10^{-1}$ mutant/cycle)[a]	fold difference[b] relative to wild-type RT	fold difference[b] V148I to Q151N
wild type[c]	1.49 ± 0.06	–	–
V148I	0.39 ± 0.03	0.3 ($p < 0.0001$)	1.5 ($p > 0.5$)
Q151N[c]	0.26 ± 0.02	0.2 ($p < 0.0001$)	–

[a] The average mutant frequency ± the standard deviation was determined from three independent experiments. [b] p values determined by χ^2 analysis. [c] Data previously published (*13*).

fidelity (for V148I and Q151N) for these mutant RTs as determined by the pre-steady state kinetic assays do indeed contribute to *in vivo* viral mutagenesis.

DISCUSSION

It is becoming more apparent that HIV-1 RT fidelity contributes to viral mutagenesis (*12*, *13*). Given that genomic hypervariability confounds both the prevention and treatment of HIV-1 infection, much research has focused on understanding the mechanisms responsible for error prone DNA polymerization by RT. One such structural element that appears to be important for the process of mutation synthesis is the binding of dNTP to amino acid residues within the RT active site. For example, mutations in residue Q151 of HIV-1 RT have been shown to increase polymerase fidelity (*10*, *16*, *31*, *32*).

Structural modeling showed that Q151 is positioned in the RT active site and directly interacts with the 3′-OH group on the sugar moiety of the incoming dNTP (*10*, *16*). When a Gln → Asn mutation is introduced at this site, the residue has a shortened side chain that may disrupt this RT−dNTP interaction. On the basis of these observations, we predicted that during correct dNTP incorporation, loss of this contact does not severely interfere with the addition of the correct dNTP. This is because alternative interactions, such as proper base pairing, stabilize the nucleotide substrate within the polymerase active site. In contrast, in the absence of proper base pairing and other interactions specific to the correct dNTP, loss of the same contact when an incorrect dNTP is present precludes misincorporation. To verify that the Q151N mutation was indeed altered in its ability to bind nucleotide substrates, we previously employed pre-steady state kinetic assays to assess how changes in this residue altered misincorporation by RT. We showed that the Q151N RT was greatly weakened in its capacity to bind incorrect dNTPs. This loss in the level of incorrect dNTP binding was sufficiently large that we were experimentally unable to measure the extent of incorrect nucleotide incorporation. These results suggested that (1) the Q151−dNTP binding interaction is a factor that contributes to the inaccurate nature of HIV-1 RT and (2) Q151N's inability to carry out misincorporation reactions may be the primary mechanism by which this mutation altered RT fidelity.

Further supporting the idea that dNTP binding is a determinant of RT fidelity are our findings for the closely related SIV system. Interestingly, an alteration in SIV RT residue 148 (Val → Ile) increased the fidelity of this polymerase (*11*). As there is no structural model available for SIV RT, we used crystallographic data of a ternary HIV-1 RT complex to generate a model for how this V148I mutation altered SIV RT fidelity (*33*). V148 resides near residue Q151 on the β8 strand of HIV-1 RT. As seen in Figure 4, unlike Q151 (red), V148 (aquamarine) does not directly interact with the incoming dNTP (purple). The side chain of V148, which lies parallel with residue Q151, makes contact with an opposing peptide backbone between residues S117 (yellow) and V118 (orange). The V148I mutation contains a longer and bulkier side chain than V148 and may push the β8 strand of RT away from the active site. This movement would disrupt the interaction between Q151 and the incoming dNTP (see two arrows in Figure 1). This model predicts that the V148I mutation disrupts the interaction between Q151 and the incoming dNTP in a manner similar to that predicted for the Q151N mutation. As a result, the V148I mutant RT would have an increased fidelity during DNA synthesis.

To test this model with the well-established HIV-1 system, one of the aims of this study was to characterize the fidelity of the V148I HIV-1 RT mutant. More specifically, since mutation synthesis is comprised of two distinct DNA polymerization events, we assessed how both the V148I and Q151N mutations affect the ability of HIV-1 RT to carry out (1) misincorporation and (2) mismatch extension events. Using the M13mp2 *lac*Zα forward mutation assay, we found that V148I RT had an 8.7-fold increase in fidelity compared to that of wild-type HIV-1 RT (Table 1). This change in fidelity is slightly smaller than that previously reported for the Q151N mutant (*16*). Given that our model predicts that the V148I mutation works via disrupting the interaction between Q151 and the incoming dNTP, it is possible that the Q151N mutation has a greater effect on RT fidelity as it directly abrogates the interaction between residue 151 and the dNTP substrate. A partial loss in the extent of the Q151−dNTP interaction may explain the intermediate change in RT fidelity observed with the V148I RT relative to the Q151N protein.

We next performed pre-steady state kinetic analyses on both these mutants to identify which step of mutation synthesis is altered by these mutations. Although we had previously measured the kinetic parameters for Q151N under misincorporation conditions, we repeated these experiments with the currently used T/P. With the new matched T/P employed in this study, which utilized correct TTP rather than correct dATP, we report that a change in either residue 148 or 151 primarily alters the ability of RT to bind (K_d) both correct and incorrect nucleotides. However, these changes in binding affinity do not alter the fidelity of the V148I RT during this first step in mutation synthesis.

As implied in eq 4 in Table 2, misinsertion fidelity assesses the ability of RT to differentiate between correct and incorrect nucleotides during the dNTP incorporation step of mutation synthesis. Given that the V148I mutation does not significantly alter the ability of the RT to execute the k_{pol} step (conformational change or catalysis) during the incorporation of either correct or incorrect dNTPs, a similar reduction in binding affinity (K_d) for these nucleotides translates into a concomitant reduction in both correct and incorrect polymerization efficiency. Consequently, the misinsertion fidelity of V148I is very similar to that of wild-type RT. These results indicate that the V148I mutation does not alter RT fidelity during the first step of mutation synthesis. While our

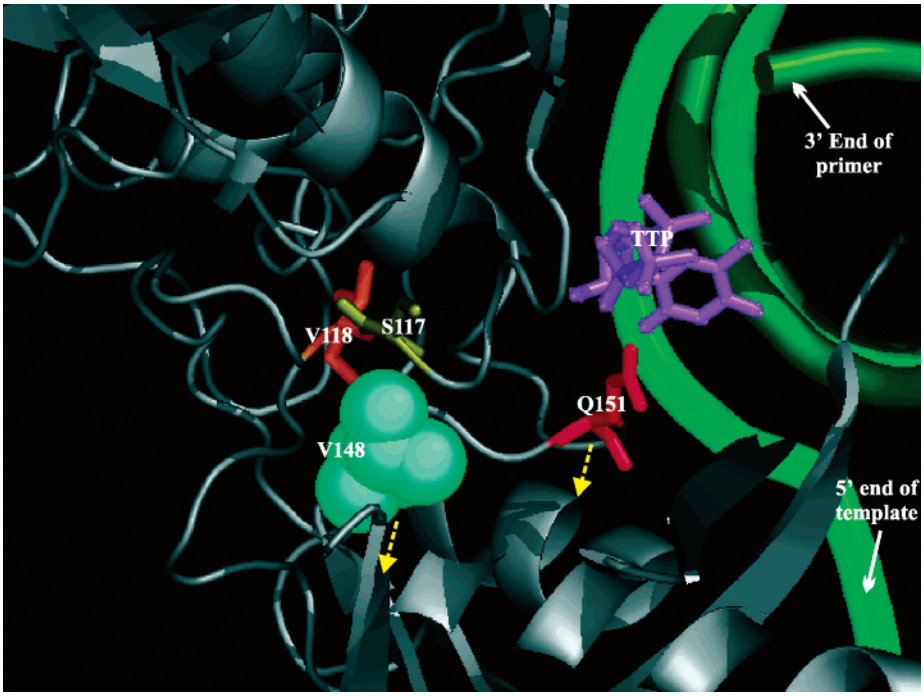

FIGURE 4: Structural model of residues V148 and Q151 of HIV-1 RT. Shown are the interactions associated with residue V148 (aquamarine) near the RT active site. This model of HIV-1 RT complexed with a T/P (green) and incoming TTP (purple) was previously generated with the program PyMOL (DeLano Scientific) using entry 1rtd from the Protein Data Bank (*11*). The side chain of V148 (aquamarine) is positioned such that it makes contact with an opposing peptide backbone between residues S117 (yellow) and V118 (orange). The yellow arrows represent the hypothetical movement of the β chain, containing both the V148 (aquamarine) and Q151 (red) residues, in the presence of the V148I mutation.

estimated values of misinsertion fidelity for the Q151N RT suggest the same, the extraordinarily low affinity of Q151N for incorrect nucleotides may limit its ability to carry out misincorporation events. One must remember the experimental conditions that are employed when polymerase fidelity is assessed. *In vitro* fidelity assays such as the M13 *lac*Zα forward mutation assay are performed with dNTP concentrations of 250 μM. Given that this concentration is significantly lower than the predicted K_d of Q151N RT for incorrect dNTPs, it is likely that this mutant RT would generally be incapable of binding these dNTPs in a manner that is productive for synthesis under the experimental conditions employed in this assay. Therefore, as described in our original Q151N model, the inability of Q151N to bind incorrect dNTPs precludes completion of misincorporation events.

To provide a complete analysis of mutation synthesis, we next assessed the pre-steady state kinetics of mismatch extension. When comparing the ability of wild-type RT to incorporate TTP onto a mismatched T/P to its ability to incorporate TTP onto a matched T/P, we found that the polymerase is less efficient at performing both K_d and k_{pol} steps during the incorporation of a nucleotide onto a mismatched primer. The active site titration curve of wild-type HIV-1 RT with the mismatch T/P generated a typical biphasic response, fast pre-steady state and slow rate-limiting steady state reactions, suggesting that the step after chemistry is rate-limiting. Interestingly, the mismatch T/P extension reactions by Q151N and V148I RTs had less biphasic curves than wild-type RT, suggesting that the step before or at the chemistry step could be rate-limiting. The great reduction in both K_d and k_{pol} values in the reactions with these mutants likely contributes to this semi-biphasic incorporation response. Possibly, these V148I and Q151N mutations produce new rate-liming steps during the mismatch extension reaction, which could lead to the increase in the mismatch extension fidelity. Indeed, as shown in Table 3, the V148I and Q151N proteins have 24.7- and 16.0-fold increases in mismatch extension fidelity, respectively, relative to that of wild-type RT. Interestingly, our results support a finding previously reported by Zinnen *et al.* (*6*) when they examined mismatch extension kinetics on a DNA template. Wild-type HIV-1 RT is able to carry out incorporation of a correct TTP onto a matched or mismatched T/P very efficiently (k_{pol}/K_d, Tables 2 and 3). In contrast, its misincorporation efficiency is lower than its mismatch extension efficiency by either 10−100- or 100−1000-fold on an RNA (Table 2) or DNA template (*6*), respectively. In our study, we show that alterations of residues 148 and 151 lower the mismatch extension efficiencies to that seen with misincorporation events (Tables 2 and 3). This suggests that V148 and Q151 are structural elements in the RT active site that promote the efficient (k_{pol}/K_d) completion of mismatch extension by HIV-1 RT.

To verify that mutations in residues 148 and 151 may contribute to viral mutagenesis, the final experiment performed in this study was a pseudotyped HIV-1 virion mutation assay. In this cell-based fidelity assay, we observed that V148I exhibits a 3.8-fold and Q151N a 5.7-fold increase in fidelity relative to that of pseudovirions encoding wild-type RT. This milder effect resulting from the V148I and Q151N RT mutations on virus mutant frequencies (compared to the m13 *lac*Zα forward mutation assay, Table 1) could be anticipated on the basis of previous studies (*13*). Significantly different *in vivo* mutation rates have been determined with different retroviruses (i.e., HIV-1, HTLV-1, BLV, and SNV), suggesting that differences in the mutation rate are

associated with differences in genetic variability (*25*). However, quantitative studies for verifying this hypothesis have not been reported. The ability of small changes in the mutation rate to alter genetic variation is dependent on small virus population sizes. Currently, the effective population size of HIV-1 *in vivo* is under debate, but there are good data supporting small population sizes in solid lymphoid tissue (*34*). It is therefore likely that RT residues that are important for nucleotide binding, V148 and Q151, can significantly contribute to HIV-1 mutagenesis *in vivo*.

Our results show that while the ability to complete misincorporation is a critical component of RT fidelity, it is necessary to examine the complete process of mutation synthesis to truly understand viral mutagenesis. The interaction between residue Q151 and the nucleotide substrate appears to be a critical factor for this process, and alterations in residues that might interfere with Q151−dNTP binding (i.e., V148I mutation) also weaken the error prone nature of this polymerase. One study that assessed the pre-steady state kinetics of mismatch extension examined the Y766S KF dNTP binding mutant (*8*). The Tyr → Ser mutation at this nucleotide binding residue did not significantly alter the ability of the polymerase to complete mismatch extension. The Y766S mutation altered polymerase fidelity by changing its kinetics during the misincorporation step of mismatch extension. These results make our findings particularly interesting as the V148I and Q151N HIV-1 RT dNTP binding mutants are uniquely affected in the second step of mutation synthesis.

The focus of many previous pre-steady state kinetic studies, such as those in which the M184V and Q151M HIV-1 RT mutants were examined, has been to identify drug resistance mechanisms (*20*, *35*). While Feng and Anderson's study did assess the misinsertion fidelity of the M184V RT mutant, the authors reported that the M184V mutation did not significantly alter the ability of the polymerase to differentiate between correct and incorrect nucleotides during the first step of mutation synthesis (*20*). Although also only measuring the kinetics for misincorporation, a study examining Y115 mutants is of interest because alterations in this residue did change the misinsertion fidelity of RT (*35*). Y115 is an HIV-1 RT dNTP binding residue that interacts with the base moiety of incoming nucleotide substrates. Mutations in this residue decrease the fidelity of the polymerase, which suggests that in wild-type RT, the role of residue Y115 is to minimize mutation synthesis. When a Tyr → Phe mutation was introduced into this position, the RT was specifically altered in its ability to bind incorrect dNTPs. This reduction in K_d for incorrect dNTPs translated into a decrease in its misinsertion fidelity. Therefore, residues V148 and Q151 differ from residue Y115 not only in the fact that their interaction with nucleotide substrates is important for mutation synthesis rather than accurate DNA polymerization but also in the mechanism by which they alter RT fidelity. Mutations in residues 148 and 151 affect the ability of the polymerase to complete mismatch extension.

In this study, we report that the ability of HIV-1 RT to bind dNTPs is an important molecular determinant that influences overall viral mutagenesis. RT mutations that alter the ability of the Q151 residue to interact with the incoming dNTP weaken the ability of the polymerase to bind both correct and incorrect nucleotides. This general loss in nucleotide recognition may stem from the fact that residue 151 makes a rather universal contact with the 3′-OH group on the sugar moiety of all incoming dNTPs. When we assessed the kinetics of two RT mutants that may have altered Q151−dNTP binding, the V148I and Q151N proteins, we found that the increased fidelity of these mutants was due to a weakened capacity to carry out the second step of mutation synthesis, mismatch extension. Whereas the huge drop in the level of binding for incorrect dNTPs during the misincorporation step suggests that the Q151N mutation may alter both steps of mutation synthesis, it is the resultant change in its mismatch kinetics that makes this a novel mutant. Although previous studies show that alterations in other dNTP-binding residues (i.e., Y115) alter RT fidelity by changing the ability of the polymerase to carry out misincorporation events, our findings suggest that the ability of RT to complete mismatch extension is also a key determinant for error prone DNA polymerization. The fact that we observe a mutant frequency change with our V148I and Q151N mutants in a cell-based fidelity assay supports the idea that RT has evolved to form this Q151−dNTP interaction as a mechanism for promoting mutation synthesis.

REFERENCES

1. Preston, B. D., Poiesz, B. J., and Loeb, L. A. (1988) Fidelity of HIV-1 reverse transcriptase, *Science 242*, 1168−1171.
2. Williams, K. J., and Loeb, L. A. (1992) Retroviral reverse transcriptases: error frequencies and mutagenesis, *Curr. Top. Microbiol. Immunol. 176*, 165−180.
3. Roberts, J. D., Preston, B. D., Johnston, L. A., Soni, A., Loeb, L. A., and Kunkel, T. A. (1989) Fidelity of two retroviral reverse transcriptases during DNA-dependent DNA synthesis in vitro, *Mol. Cell. Biol. 9*, 469−476.
4. Kunkel, T. A. (1992) DNA replication fidelity, *J. Biol. Chem. 267*, 18251−18254.
5. Johnson, K. A. (1993) Conformational coupling in DNA polymerase fidelity, *Annu. Rev. Biochem. 62*, 685−713.
6. Zinnen, S., Hsieh, J. C., and Modrich, P. (1994) Misincorporation and mispaired primer extension by human immunodeficiency virus reverse transcriptase, *J. Biol. Chem. 269*, 24195−24202.
7. Kati, W. M., Johnson, K. A., Jerva, L. F., and Anderson, K. S. (1992) Mechanism and fidelity of HIV reverse transcriptase, *J. Biol. Chem. 267*, 25988−25997.
8. Carroll, S. S., Cowart, M., and Benkovic, S. J. (1991) A mutant of DNA polymerase I (Klenow fragment) with reduced fidelity, *Biochemistry 30*, 804−813.
9. Wong, I., Patel, S. S., and Johnson, K. A. (1991) An induced-fit kinetic mechanism for DNA replication fidelity: direct measurement by single-turnover kinetics, *Biochemistry 30*, 526−537.
10. Weiss, K. K., Bambara, R. A., and Kim, B. (2002) Mechanistic role of residue Gln151 in error prone DNA synthesis by human immunodeficiency virus type 1 (HIV-1) reverse transcriptase (RT). Pre-steady state kinetic study of the Q151N HIV-1 RT mutant with increased fidelity, *J. Biol. Chem. 277*, 22662−22669.
11. Diamond, T. L., Souroullas, G., Weiss, K. K., Lee, K. Y., Bambara, R. A., Dewhurst, S., and Kim, B. (2003) Mechanistic understanding of an altered fidelity simian immunodeficiency virus reverse transcriptase mutation, V148I, identified in a pig-tailed macaque, *J. Biol. Chem.* (in press).
12. O'Neil, P. K., Sun, G., Yu, H., Ron, Y., Dougherty, J. P., and Preston, B. D. (2002) Mutational analysis of HIV-1 long terminal repeats to explore the relative contribution of reverse transcriptase and RNA polymerase II to viral mutagenesis, *J. Biol. Chem. 277*, 38053−38061.
13. Mansky, L. M., Le Rouzic, E., Benichou, S., and Gajary, L. C. (2003) Influence of reverse transcriptase variants, drugs, and Vpr on human immunodeficiency virus type 1 mutant frequencies, *J. Virol. 77*, 2071−2080.
14. Kim, B., Hathaway, T. R., and Loeb, L. A. (1996) Human immunodeficiency virus reverse transcriptase. Functional mutants obtained by random mutagenesis coupled with genetic selection in *Escherichia coli*, *J. Biol. Chem. 271*, 4872−4878.

15. Kim, B. (1997) Genetic selection in *Escherichia coli* for active human immunodeficiency virus reverse transcriptase mutants, *Methods 12*, 318−324.
16. Weiss, K. K., Isaacs, S. J., Tran, N. H., Adman, E. T., and Kim, B. (2000) Molecular architecture of the mutagenic active site of human immunodeficiency virus type 1 reverse transcriptase: roles of the beta 8-alpha E loop in fidelity, processivity, and substrate interactions, *Biochemistry 39*, 10684−10694.
17. Bebenek, K., and Kunkel, T. A. (1995) Analyzing fidelity of DNA polymerases, *Methods Enzymol. 262*, 217−232.
18. Johnson, K. A. (1995) Rapid quench kinetic analysis of polymerases, adenosine triphosphatases, and enzyme intermediates, *Methods Enzymol. 249*, 38−61.
19. Kerr, S. G., and Anderson, K. S. (1997) Pre-steady-state kinetic characterization of wild type and 3′-azido-3′-deoxythymidine (AZT) resistant human immunodeficiency virus type 1 reverse transcriptase: implication of RNA directed DNA polymerization in the mechanism of AZT resistance, *Biochemistry 36*, 14064−14070.
20. Feng, J. Y., and Anderson, K. S. (1999) Mechanistic studies examining the efficiency and fidelity of DNA synthesis by the 3TC-resistant mutant (184V) of HIV-1 reverse transcriptase, *Biochemistry 38*, 9440−9448.
21. Suo, Z., and Johnson, K. A. (1997) Effect of RNA secondary structure on the kinetics of DNA synthesis catalyzed by HIV-1 reverse transcriptase, *Biochemistry 36*, 12459−12467.
22. Mansky, L. M., and Temin, H. M. (1995) Lower in vivo mutation rate of human immunodeficiency virus type 1 than that predicted from the fidelity of purified reverse transcriptase, *J. Virol. 69*, 5087−5094.
23. Mansky, L. M. (1996) Forward mutation rate of human immunodeficiency virus type 1 in a T lymphoid cell line, *AIDS Res. Hum. Retroviruses 12*, 307−314.
24. Landau, N. R., Page, K. A., and Littman, D. R. (1991) Pseudotyping with human T-cell leukemia virus type I broadens the human immunodeficiency virus host range, *J. Virol. 65*, 162−169.
25. Mansky, L. M. (2000) In vivo analysis of human T-cell leukemia virus type 1 reverse transcription accuracy, *J. Virol. 74*, 9525−9531.
26. Ito, W., Ishiguro, H., and Kurosawa, Y. (1991) A general method for introducing a series of mutations into cloned DNA using the polymerase chain reaction, *Gene 102*, 67−70.
27. Mansky, L. M. (1996) The mutation rate of human immunodeficiency virus type 1 is influenced by the vpr gene, *Virology 222*, 391−400.
28. Vaccaro, J. A., Singh, H. A., and Anderson, K. S. (1999) Initiation of minus-strand DNA synthesis by human immunodeficiency virus type 1 reverse transcriptase, *Biochemistry 38*, 15978−15985.
29. Thrall, S. H., Krebs, R., Wohrl, B. M., Cellai, L., Goody, R. S., and Restle, T. (1998) Pre-steady-state kinetic characterization of RNA-primed initiation of transcription by HIV-1 reverse transcriptase and analysis of the transition to a processive DNA-primed polymerization mode, *Biochemistry 37*, 13349−13358.
30. Yu, H., and Goodman, M. F. (1992) Comparison of HIV-1 and avian myeloblastosis virus reverse transcriptase fidelity on RNA and DNA templates, *J. Biol. Chem. 267*, 10888−10896.
31. Sarafianos, S. G., Pandey, V. N., Kaushik, N., and Modak, M. J. (1995) Glutamine 151 participates in the substrate dNTP binding function of HIV-1 reverse transcriptase, *Biochemistry 34*, 7207−7216.
32. Harris, D., Kaushik, N., Pandey, P. K., Yadav, P. N., and Pandey, V. N. (1998) Functional analysis of amino acid residues constituting the dNTP binding pocket of HIV-1 reverse transcriptase, *J. Biol. Chem. 273*, 33624−33634.
33. Huang, H., Chopra, R., Verdine, G. L., and Harrison, S. C. (1998) Structure of a covalently trapped catalytic complex of HIV-1 reverse transcriptase: implications for drug resistance, *Science 282*, 1669−1675.
34. Frost, S. D., Dumaurier, M. J., Wain-Hobson, S., and Brown, A. J. (2001) Genetic drift and within-host metapopulation dynamics of HIV-1 infection, *Proc. Natl. Acad. Sci. U.S.A. 98*, 6975−6980.
35. Ray, A. S., Basavapathruni, A., and Anderson, K. S. (2002) Mechanistic studies to understand the progressive development of resistance in human immunodeficiency virus type 1 reverse transcriptase to abacavir, *J. Biol. Chem. 277*, 40479−40490.

BI035258R